NIH Public Access
Author Manuscript
Dev Biol. Author manuscript; available in PMC 2013 June 24.

Published in final edited form as:
Dev Biol. 2009 August 15; 332(2): 360–370. doi:10.1016/j.ydbio.2009.06.003.

Collagen IX is required for the integrity of collagen II fibrils and the regulation of vascular plexus formation in Zebrafish caudal fins

Cheng-chen Huang[a,*,1], **Tai-Chuan Wang**[a,2], **Bo-Hung Lin**[a,b,2], **Yi-Wen Wang**[a], **Stephen L. Johnson**[c], and **John Yu**[a,d,*]

[a]Institute of Cellular and Organismic Biology, Academia Sinica, 128 Academia Road, Section 2, Nankang, Taipei 115, Taiwan

[b]Institute of Bioscience and Biotechnology, National Taiwan Ocean University, Keelung, Taiwan

[c]Department of Genetics, Washington University Medical School, St. Louis, MO, USA

[d]Genomics Research Center, Academia Sinica, Taipei, Taiwan

Abstract

Capillary plexuses form during both vasculogenesis and angiogenesis and are remodeled into mature vessel types and patterns which are delicately orchestrated with the sizes and shapes of other tissues and organs. We isolated a zebrafish mutation named *prp* (for *persistent plexus*) that causes persistent formation of vascular plexuses in the caudal fins and consequent mispatterning of bony fin rays and the fin shape. Detailed analyses revealed that the *prp* mutation causes a significant reduction in the size and dramatic structural defects in collagen II-rich extracellular matrices called actinotrichia of both embryonic finfolds and adult fins. *prp* was mapped to chromosome 19 and found to encode the zebrafish collagen9α1 (col9α1) gene which is abundantly expressed in developing finfolds. A point mutation resulting in a leucine-to-histidine change was detected in the thrombospondin domain of the col9α1 gene in *prp*. Morpholino-mediated knockdown of col9α1 phenocopied the *prp* small-finfold phenotype in wild-type embryos, and an injection of plasmids containing the col9α1 cDNA into *prp* embryos locally restored the finfold size. Furthermore, we found that osteoblasts in *prp* mutants were mispatterned apparently following the abnormal vascular plexus pattern, demonstrating that blood vessels play an important role in the patterning of bony rays in zebrafish caudal fins.

Keywords

Zebrafish; Vascular plexus; Collagen IX; Actinotrichia; Fin

Introduction

The patterning of peripheral body parts that creates the unique sizes and shapes of different species is a fascinating phenomenon to many biologists (Lecuit and Le Goff, 2007). Unlike

© 2009 Elsevier Inc. All rights reserved.

*Corresponding author. Fax: + 886 2 2789 9503., cheng-chen.huang@uwrf.edu (C. Huang), johnyu@gate.sinica.edu.tw (J. Yu)..
[1]Present address: Department of Biology, University of Wisconsin-River Falls, River Falls, WI 54022, USA.
[2]These authors contributed equally to this work.

Appendix A. Supplementary data

Supplementary data associated with this article can be found, in the online version, at doi:10.1016/j.ydbio.2009.06.003.

NIH-PA Author Manuscript
NIH-PA Author Manuscript
NIH-PA Author Manuscript

NIH-PA Author Manuscript

NIH-PA Author Manuscript

NIH-PA Author Manuscript

genetic mechanisms of the fundamental anterior–posterior, dorsal–ventral, and left– right body axes that have been found in the past few decades to be amazingly conserved among species and to involve the interplay of numerous signaling pathways (Meinhardt, 2008), our understanding of the mechanisms for patterning of peripheral body parts, such as insect wings, fish fins, and rodent limbs, is still very limited (Lecuit and Le Goff, 2007). One of the major challenges is that it is hard to dissect out the contribution of a specific gene or pathway in the patterning process due to the fact that the development of these tissues and organs normally involves complicated interactions of multiple tissues and often requires physiological support from the vascular system. For example, blood vessels are known to induce the differentiation and proliferation of organ primordia by emitting and/ or transporting morphogens or growth factor(s), to sustain organogenesis by providing blood circulation, and even to govern organ patterning by yet unclear mechanisms (Cleaver and Melton, 2003; Lammert et al., 2001). Conversely, growing organs/tissues typically send out angiogenic factors to induce the proliferation, migration, and even modeling of blood vessels into delicate vascular patterns to facilitate organ and tissue growth (Crivellato et al., 2007). With such complicated relationships, it is extremely difficult to determine what the primary cause of a malformed body part or organ is. Nonetheless, it is clear that blood vessels not only play a vital role in controlling the formation of many late-developing organs and tissues in normal conditions, but that they are also crucial for pathological development. In cancer biology, it has been well documented that blood vessel growth into tumor tissues is essential for both tumor growth and metastasis (Carmeliet, 2005). This relationship has inspired the idea of applying antiangiogenesis therapies for cancer, which has already produced encouraging results in both laboratory and clinical settings (Ferrara and Kerbel, 2005). While the importance of blood vessels in organ/tissue patterning can be readily appreciated in those studies, a tractable model system to observe and track the amazingly intricate developmental processes and interactions between peripheral body parts and blood vessels is still lacking.

Among the numerous interactions taking place between developing tissues and blood vessels, the interaction between vascular endothelial cells (ECs) and the extracellular matrix (ECM) surrounding developing tissues has been gaining the attention of vascular biologists. Studies have revealed that ECM proteins which were previously considered to be structural proteins have been found to actively participate in several aspects of angiogenesis and organogenesis (Davis and Senger, 2005). For example, accumulating evidence has shown that both proliferation and survival of ECs are highly dependent on the adhesion of ECs to the ECM (Meredith and Schwartz,1997;Aplin et al., 1999; Senger et al., 2002). ECMs can regulate cell migration by establishing haptotatic gradients of ECM proteins for vascular ECs (Senger et al., 2002). The ECM also influences vascular patterning. Some ECM proteins such as collagen I bind to and promote behavioral changes in ECs, but not fibroblasts, which resemble precapillary cord formation observed during embryonic vasculogenesis (Montesano et al., 1983; Whelan and Senger, 2003). More recently, ECM molecules were found to directly bind to growth factors for blood vessel growth, such as vascular endothelial growth factors (VEGFs), hepatocyte growth factor (HGF), and keratinocyte growth factor, to regulate tube formation and the proliferation of ECs (Ruehl et al., 2002; Wijelath et al., 2002; Rahman et al., 2005). Despite these findings, it is still challenging to precisely define the roles of specific ECM components in the development of blood vessels and the subsequent development of adjacent organs and body parts, due to the numerous members, large sizes, and diverse structures of the ECM.

Collagen is one of the major components of the ECM. Among the identified 27 different types of collagens, collagen IX is a heterotrimeric non-fibrillar collagen composed of three α chains, collagen 9α1 (col9α1), col9α2, and col9α3, which are encoded by three different genes (Canty and Kadler, 2005). Collagen IX contains three collagenous and four non-

NIH-PA Author Manuscript

NIH-PA Author Manuscript

NIH-PA Author Manuscript

collagenous domains and is thought to serve as a bridge between collagens and/or non-collagenous matrix proteins (Diab et al., 1996). Knockout of the col9α1 gene in mice causes no morphological defects at birth, but progressively degenerative joints in mice aged 4 months and older (Fässler et al., 1994). In humans, mutations of col9α2 and col9α3 were respectively found to be associated with intervertebral disc and lumbar disc diseases (Annunen et al., 1999; Paassilta et al., 2001). While gene knockout and human genetic studies have provided evidence supporting collagen IX being a connecting element in ECM networks, it was interesting to note that col9α1 is one the few collagen chains that contains a thrombospondin domain. The thrombospondin domain of human col9α1, for example, is a non-helical structure containing about 245 amino acids located N-terminal to the triple helix (Bork, 1992). The current model suggests that collagen IX molecules bind to other collagen fibrils through its helix domain leaving the N-terminal domain projecting out to interact with other matrix proteins (Eyre et al., 2006). Thrombospondins from which the thrombospondin domain was originally identified have been shown to bind various angiogenic factors and are implicated, in most but not all studies, in antiangiogenesis (Streit et al., 1999; Armstrong and Bornstein, 2003; Margosio et al., 2003). Therefore, our understanding of how collagen IX functions is still limited, and to our knowledge, no study has ever addressed or examined the roles of collagen IX in angiogenesis.

In this report, we utilized zebrafish to study the patterning of one of the peripheral body parts, the caudal fin, during normal and regenerative development. With our forward genetic approach, we identified a mutation named *prp* (for *persistent plexus*), which shows persistent formation of vascular plexuses in normally developing and regenerating fins. *prp* was found to be located on the zebrafish col9α1 gene, and the mutation occurs in the thrombospondin domain of the protein. Our phenotypic analyses provided evidence that zebrafish collagen IX is also required for the integrity of ECM structure such as actinotrichial matrices, which had a disintegrated appearance in mutants. The striking vascular plexus phenotypes of *prp* illustrate for the first time that collagen IX is involved in regulating the formation of vascular plexuses during angiogenesis. Furthermore, our results demonstrate zebrafish caudal fins to be a well-tractable genetic model for studying the patterning of peripheral body parts as well as interactions between blood vessels and neighboring tissues during development.

Materials and methods

Zebrafish husbandry and breeding

The zebrafish stocks used in this study were maintained following standard procedures (Westerfield, 2000) and were bred by in *vitro* fertilization. *prp* is a homozygous viable mutation maintained in the TG(*fli1:EGFP*)^{y1} background which was originally derived from the AB inbred line. SJD is another inbred zebrafish line the genetic background of which has been shown to greatly differ from the AB line and thus is regularly used for PCR-based mapping (Johnson et al., 1994).

Mutagenesis and isolation of prp

Random mutagenesis was carried out at Washington University School of Medicine, St. Louis, MO, USA with wild-type TG(*fli1:EGFP*)^{y1} transgenic fish following standard protocols (Solnica-Krezel et al., 1994). In brief, 30 homozygous male fish at 3–4 months old were treated with 3 mM of ethylnitrosolurea (ENU) for 1 h. The same treatment was repeated for a total of four times separated by 10-day intervals. Treated fish were allowed to rest for 1 month before being outcrossed to untreated females to generate a large stock of so-called F1 funders. When mature, the F1 females were used for mutant screening. We adopted an early pressure protocol for our screening (Streisinger et al., 1981). In brief, eggs

NIH-PA Author Manuscript

NIH-PA Author Manuscript

NIH-PA Author Manuscript

were gently expelled from F1 females and fertilized with UV-treated sperm. Soon after fertilization, embryos were transferred to a glass bottle with a rubber cap, placed in a water-filled cylinder, and 8000 psi (pounds per square inch) of pressure was applied to the water for 150 s through a pistol using a traditional French Press. After applying the hydrostatic pressure, gynogenetic diploid embryos were carefully transferred to a 6-cm dish and raised using standard procedures. Fin regeneration was examined in gynogenetic adult fish, and F1 carriers were outcrossed to generate an F2 stock which was then intercrossed to recover the mutation. After two outcrosses, the *prp* mutants showed consistent fin phenotypes with no sign of the presence of a second mutation in the *prp* background. *prp*-heterozygous fish developed normal fins.

Mapping and cloning of prp

The *prp* mutation was first outcrossed to the SJD zebrafish strain to generate a hybrid stock. Male heterozygous hybrid fish were then backcrossed to *prp* females, and the progeny were used for the 1st pass linkage mapping by taking advantage of the much-lower recombination rate in males (Singer et al., 2002). With 24 male meiotic individuals, although normally 12 would be sufficient, *prp* was first found to be linked to the simple sequence length polymorphism (SSLP) marker, z3782, of chromosome 19 (two recombinants), while markers for the other chromosomes showed clear results of no linkage (with around 12 recombinants). Next, fine mapping was carried out with female meiotic individuals, i.e., progeny from crosses between female hybrid fish and male *prp* mutants until a small critical region was identified. Candidate genes within the *prp* critical region, about five–seven genes based on the Zv_6 assembly, were cloned by reverse-transcriptase polymerase chain reaction (RT-PCR), and *in situ* hybridizations were carried out on them. For some genes, we further performed 5′- and 3′-RACE experiments to uncover the full length of their cDNAs.

Constructs for overexpressing col9α1 and microinjections

Complementary (c)DNA of the col9α1 coding region was amplified and TA-cloned into the pcDNA3.1/V5-His-TOPO vector designed to express proteins with V5 and 6-histidine double fusions at the C-terminal under the cytomegalovirus (CMV) promoter (Invitrogen, Carlsbad CA), and 50–200 pg of plasmids from several independent clones were injected into 1–2-cell-stage *prp* embryos. The finfolds of injected embryos were measured at 2 and 3 days post-fertilization (dpf). Primers were 5′ AGGTCGTCCTCAGTCAGAGAGG and 3′ GCTGCCCTGCTGGATCACACTG.

Microinjection was performed with a microinjector Nanoject II (Drummond Scientific, Broomall PA). We normally injected 2.3 nl of the diluted morpholino or RNA or a mixture of both into embryos at the 1–2-cell stage, which were then analyzed with a Leica MFIII stereo fluorescent microscope and Leica TCS-SP5 confocal microscope. The morpholino sequence for col9α1 was TCAGAGTGTGGAGTCTCACCACTAC.

Immunohistochemistry and in situ hybridization

Embryos were fixed in 4% paraformaldehyde overnight at 4 °C for *in situ* hybridization and immunohistochemistry. For immunohistochemistry, fixed embryos were washed twice with phosphate-buffered saline (PBS), then once with H_2O for 5 min each, and permeabilized with −20 °C acetone for 7 min followed by washes in H_2O and then PBS. Embryos were incubated in 3% bovine serum albumin (BSA) in PBST (PBS and 0.1% Tween 20) for at least 1 h at room temperature before an overnight incubation with the monoclonal antibody (mAb) for type II collagen in PBST (II-II6B3, 1:10 dilution, Developmental Studies Hybridoma Bank, Iowa City, IA, USA) at 4 °C. The next day, embryos were washed with PBST at least four times for 15 min each. After that, embryos were incubated with a cy3-conjugated anti-mouse immunoglobulin G (IgG) secondary antibody (1:800, Jackson

NIH-PA Author Manuscript

NIH-PA Author Manuscript

NIH-PA Author Manuscript

ImmunoResearch Laboratories, West Grove, PA, USA) for 2 h at room temperature. At the end of the secondary antibody incubation, embryos were washed with PBST several times before being transferred to Vectashield mounting media from Vector Laboratories (Burlingame, CA, USA). Whole-mount *in situ* hybridization was carried out with an InsituPro VS robot by Intavis Bioanalytical Instruments (Koln, Germany) following the manufacturer's standard procedures. Vital dye staining with calcein for fin rays was performed according to the protocol described by Du et al. (2001).

Transmission electron microscopy (TEM)

Embryos were fixed in 2% glutaraldehyde, 2% paraformaldehyde, and 0.1 M sodium phosphate (pH 7.4) overnight at 4 °C followed by post-fixing with 1% OsO_4 for 1 h at room temperature. Fixed embryos were then dehydrated by an ethanol series with the following steps: 30% for 10 min, 50% for 10 min, 70% for 20 min, 80% for 20 min, 90% for 20 min, 95% for 20 min, 100% ethanol for 60 min, and then twice in xx% acetone for 30 min each. Infiltration was carried out with a 1:1 ratio of resin:acetone for >12 h, 2:1 of resin: acetone for >12 h, pure resin >12 h, and one more time with pure resin overnight. Embryos were embedded in a 70 °C oven overnight. The plastic blocks were then trimmed and sectioned to obtain 1-μm or ultrathin sections of 70–90 nm which were collected on 200-mesh copper grids and stained with uranyl acetate for 50 min and lead citrate for 10 min. Sections were analyzed with a Hitachi H-7000 transmission electron microscope.

Results

The zebrafish prp mutation causes persistent formation of vascular plexuses at fin tips

We took the forward genetic approach to initially study the mechanisms of blood vessel regeneration in zebrafish. Using the transgenic *TG(fli1:EGFP)*^{y1} zebrafish which expresses EGFP in all endothelial cells and thus marks the vasculature nicely in the fins (Lawson and Weinstein, 2002), we previously reported transient vascular plexus formation during blood vessel regeneration in the zebrafish caudal fin (Huang et al., 2003). The formation of vascular plexuses in regenerating fins normally appears only between 3 and 8 days post-amputation (dpa; Huang et al., 2003). In an ENU-based mutant screening (see “Materials and methods” for details), we isolated a recessive mutation named *prp* (for persistent plexus) that shows defects in regulating vascular plexus formation. Homozygous mutants are viable, fertile, and morphologically indistinguishable from the wild-type (WT) (Figs. 1A, B). However, all the regenerating fins in *prp* mutants are smaller and have slightly rounded edges after amputations. When we examined the regenerating blood vessels, *prp* formed normal vascular plexuses during the plexus formation stage of blood vessel regeneration (Figs. 1C, D) but continued to form vascular plexuses at the distal tips of the regenerating fins after 10 dpa when WT fish ceased plexus formation (Figs. 1E, F). In addition, the *prp* mutation also caused plexus formation in un-amputated fins. In WT fish, blood vessels typically formed two simple U-shaped connections at the tip of each fin ray (Fig. 1G). We found relatively denser blood vessel networks in normal *prp* fin tips (Fig. 1H). Thus, *prp* is likely to be a negative regulator of vascular plexus formation in the zebrafish caudal fin, as *prp* mutants form plexuses during ontogenetic and late regenerative angiogenesis when plexuses normally do not form.

Small finfolds and vascular plexuses in young caudal fins of prp mutants

To investigate the developmental defects underlying persistent plexus formation with the *prp* mutation, we examined early vascular morphogenesis of young caudal fins. In the WT, the caudal fin is derived from a precursor structure called the finfold which is a thin avascular tissue for swimming formed along the ventral, dorsal, and caudal edges of the trunk during embryonic and larval stages (Akimenko et al., 1995) (Figs. 2A, C; only the caudal finfold is

NIH-PA Author Manuscript

NIH-PA Author Manuscript

NIH-PA Author Manuscript

shown). At about 2 weeks of age, time-lapse images showed that fin blood vessels begin to branch out from the posterior ends of the axial vessels towards the ventral caudal aspect of the finfolds (Fig. 2E). Within 2 days, these pioneer blood vessels extensively branch and soon arrange themselves into the fin ray pattern (Figs. 2F, G). The blood vessels continue to grow dorsally and ventrally to a total number of 16 or 18 rays with the adult fin vasculature in the next few days while maintaining nicely separated vessel pairs for each fin ray (Fig. 2H).

In *prp* mutants, we first noted that the embryonic finfold was only half the size of that of the WT (Figs. 2A, B; see measurements in Fig. 4A). This phenotype persisted for 2–3 weeks (Fig. 2D) until the finfolds were transformed into caudal fins, at which time *prp* began to show the vascular plexus phenotype (Figs. 2I – L). Fin vessels in *prp* mutants also grew from the posterior ends of the axial vessels into the finfolds at about the same time as did the WT (Figs. 2I, J) but soon formed vascular plexuses where dense vessels networks could readily be perceived (Fig. 2K). The *prp* vascular plexuses then apparently underwent remodeling and formed a ray-like pattern. Closer examination of these vessels revealed that most of them were irregularly separated and sometimes juxtaposed and formed abnormal connections (Fig. 2L; more analyses below). Furthermore, these vessels were often accompanied by wavy or fused bony fin rays or lepidotrichia, which could be visualized by the vital dye, calcein (arrows in Figs. 2N, P; Du et al., 2001). Ray fusion actually occurred at the base of the lepidotrichia where the lepidotrichia were connected to the radial plates (Fig. S1). Similar wavy lepidotrichia were also observed in the dorsal and anal fins (Fig. S1).

prp encodes for the zebrafish col9α1 gene

We first carried out positional cloning for *prp* using 24 male meiotic individuals (see “Materials and methods” for details) to determine that *prp* is on linkage group 19 (Fig. 3A). Next, we generated a panel of approximate 1900 female meiotic individuals for fine mapping. *prp* was then mapped to the area between z4825 and z3782 polymorphic markers (Fig. 3A). We further narrowed down *prp* to a critical region near the junction of the Zv_6 scaffolds 2791 and 2792 with 2 and 9 recombinations between *prp* and the left and right marginal markers, respectively (Fig. 3A). Within this critical region, a number of collagen genes were predicted. We tested the candidacy of these genes first by in situ hybridization and found that only col22α1 and col9α1 were expressed in the finfolds (Figs. 3B, C and data not shown). Col9α1 was also highly expressed in the finfold of 2-dpf embryos (Fig. 3D) and in the developing caudal fins (Fig. 3E) where col22α1 was only weakly expressed (Figs. S2A, B). In regenerating fins, col9α1 was more abundantly expressed than col22α1 at the growing fin tips (Figs. S2C, D). Cross-sections show that indeed col9α1 was expressed in cells surrounding the area where the matrix structures called actinotrichia were being formed (Fig. 3H; more analyses of actinotrichia are given below and see Fig. 5E), whereas col22α1 was expressed in a subset of the col9α1-expressing cells (Fig. S2). Thus, the analyses with *in situ* hybridization suggested that both col9α1 and col22α1 are candidates for *prp*.

The full-length cDNAs of col22α1 and col9α1 of WT and *prp* mutants were sequenced. While no nucleotide change was detected in col22α1 cDNA, a T-to-A mutation was detected in the col9α1 gene of *prp* causing a leucine (176)-to-histidine amino-acid change (Fig. 3F). The point mutation also created a restriction enzyme site for ApaLI in the col9α1 gene of *prp* which was verified by ApaLI enzyme digestion on a small piece of cDNA covering the mutation site (Fig. 3G). The zebrafish col9α1 gene is composed of at least 36 exons and translates into a 942-amino-acid-long protein (Fig. 3I). The protein contains a thrombospondin domain at the N terminus followed by a short gap and then numerous typical glycine-X–Y repeats found in collagens (Fig. 3J). The point mutation of *prp* occurred in the 5th exon which encodes for the thrombospondin domain. In addition, we found that

NIH-PA Author Manuscript

NIH-PA Author Manuscript

NIH-PA Author Manuscript

the leucine (176) residue is conserved in the thrombospondin domain of col9α1 in human, mouse, and many other species suggesting its important role in col9α1 function (data not shown).

A morpholino targeting the 3′ splice site of exon 5 of the zebrafish col9α1 gene was designed to test whether knockdown of this gene can phenocopy the early finfold phenotype of *prp* when injected into WT embryos. This morpholino was designed to block the splice site and consequently delete exon 5 and generate an early stop codon in exon 6. In this experiment, we compared the sizes of finfolds of 2-dpf embryos. While the finfolds of uninjected embryos grew to 150 μm in length, those injected with 5 ng of the col9α1 morpholino were only 100 μm on average (Figs. 4A, B and D; $p<0.0001$, $n=37$ WT, 24 morphants). Homozygous *prp* mutants showed small finfolds as well (Figs. 4A, C; $n=34$). Next, we tested whether overexpression of col9α1 was able to rescue the finfold phenotype of *prp*. We injected 50–200 pg of plasmids containing the entire coding sequence of col9α1 into *prp* embryos. The results showed that some *prp* embryos (11/50) developed an extra portion of finfolds with normal-looking actinotrichia which is the main collagen structure in finfolds (Fig. 4E and more below), suggesting that overexpression of col9α1 can locally rescue *prp* finfolds. Together, these results strongly suggest that *prp* encodes the zebrafish col9α1 gene.

Ultrastructure of the developing fin in wild-type zebrafish

To further understand the cellular defects underlying the *prp* phenotypes, we first analyzed the fin structure of wild-type in details. Finfolds of teleosts are typically comprised of type II collagen matrix structures called actinotrichia which are laterally sandwiched between the epidermis (Wood and Thorogood, 1984). As the caudal finfolds continue to develop and transform into the caudal fins, actinotrichia are gradually replaced by lepidotrichia, another collagen-rich matrix structure, and the actinotrichia only exist at the distal tip of each fin ray in mature fins (detail below). Closer examination with transmission electron microscopy (TEM) revealed several interesting differences between the two major exoskeletal structures (Figs. 5 and 6; Johanson et al., 2005). First, while actinotrichia exhibit a compact collagen bundle lepidotrichia appear to have a relatively loose matrix structure (Figs. 5A–C). Longitudinal sections of TEM reveal the typical collagen striation pattern of actinotrichia (Fig. 6F) but not of lepidotrichia (Fig. 5A and data not shown). Second, actinotrichia bundles appear to have different sizes, with some large ones close to the size of a cell, suggesting a very dynamic assembly process for it. Lepidotrichia, on the other hand, form a crescent matrix that grows thicker and eventually turns into the two mature hemi fin rays enclosing the mesenchymal cells (Figs. 5A, B). Third, they are assembled at different locations and by different cells. At the very distal tip, while no lepidotrichia could be found, actinotrichia are formed between epidermis and the single layer of mesenchymal cells (Fig. 5C). At a medial level, actinotrichia now are sandwiched between the two arrays of mesenchymal cells presumably fibroblasts which express col9α1 (Fig. 5B; also see Fig. 3H) while lepidotrichia are formed between the epidermis and the adjacent osteoblasts (Figs. 5A, B, arrows). At a more proximal level, the number of actinotrichia bundle is decreasing while lepidotrichia is growing thicker (Fig. 5A). All these suggest that the two major collagen-containing matrices in the zebrafish caudal fins are formed by different mechanisms.

Small and disintegrated actinotrichia in prp mutants

We went on to examine the fin structure of *prp*. We first noticed that, under bright light, while actinotrichia in wild-type finfolds appear as tiny brightly reflected radial lines (Fig. 6A; Mabee 1988) those in *prp* mutants were often thinner, misoriented, or even absent (Fig. 6B). Second, immunohistochemical studies using the mAb for type II collagen showed that WT embryos developed dense collagen II-rich actinotrichia in the finfolds, but *prp* mutants

NIH-PA Author Manuscript

NIH-PA Author Manuscript

NIH-PA Author Manuscript

usually had short and disrupted actinotrichia (Figs. 6C, D). TEM analyses revealed that the actinotrichia of *prp* fins indeed were strikingly smaller and disintegrated and had snowflake-like appearance (arrows in Figs. 5E, F and asterisks in Figs. 6F, G). Occasionally, some actinotrichia were assembled in a perpendicular orientation (arrow in Fig. 6F) or penetrated lepidotrichia (arrows in Fig. 6H). Thus, a mutation in the thrombospondin domain of col9α1 caused defects in the integrity and patterning of actinotrichia in zebrafish fins.

The vascular pattern guides the osteoblast pattern in fins

We described above the vascular plexuses and fused bony fin ray phenotypes of *prp*. To understand the relationship between these two phenotypes of the *prp* mutation, we examined lepidotrichia patterning in young caudal fins. Our time course examinations revealed that lepidotrichia developed later than blood vessels in the fin and appeared to be closely associated with blood vessels soon after they became visible under a microscope (Fig. S3). At that time, blood vessels had already grown into a larger area of the caudal fin, where few or no lepidotrichia could be detected. This association also occurred in *prp* mutants, and the lepidotrichia appeared to be associated with stray blood vessels (Fig. S3). Second, we utilized the ZnS5 mAb which recognizes osteoblasts and found that in WT fish, osteoblasts were detected by ZnS5 later than blood vessels in the caudal fin (Figs. 7D, E). Soon after the blood vessels had developed into the caudal fin, we often observed no osteoblasts in most dorsal and ventral areas of young caudal fins where blood vessels were already present (arrow in Fig. 7E). At a later time, ZnS5-positive cells formed the ray pattern that was closely associated with vessel rays, suggesting that osteoblast rays which later form lepidotrichia are guided by vessel patterning. In support of this idea, osteoblasts in *prp* mutants, which also appeared later than blood vessels, formed crooked or fused rays that were associated with abnormally connected blood vessels (Figs. 7G–I). These results strongly suggest that blood vessels guide osteoblast patterning in zebrafish caudal fins. Thus, the lepidotrichia defect is likely secondary to blood vessel mispatterning in *prp* mutants. In the chicken, sensory neurons were found to guide blood vessel patterning (Mukouyama et al., 2002). We examined neuronal axons with the Zn8 mAb and found that the axon patterning in *prp* was relatively normal and did not seem to be associated with vascular plexuses, suggesting that the vessel plexus phenotype was not due to axon mispatterning (Figs. 8A, B). Finally, we examined the relationship between the developing epidermis, which was also labeled by the Zn8 antibody, and blood vessels in the caudal fins. We found that the epidermal pattern appeared indistinguishable between WT and *prp* mutants (Figs. 8C, D) suggesting an independent relationship between the epidermal and blood vessel patterning in zebrafish caudal fins.

Discussion

The new role of collagen IX in angiogenesis

Our studies on the zebrafish *prp* mutation led us to discover a new role for collagen IX in vascular development. In particular, our results suggest that collagen IX regulates the formation of vascular plexuses in developing peripheral body parts that involve a significant amount of the ECM. In col9α1 mutants, vascular plexuses formed in developing young fins and later in the fin tips (Figs. 1, 2). The abnormally dense vascular networks in *prp* mutants did not seem to result from overproliferation of ECs, as we found similar numbers of ECs in *prp* mutants as in WT fish when the plexus was formed (data not shown). This did not likely result from over-branching of blood vessels either, because when we crossed *prp* into another zebrafish mutation named *reg6*, which was shown to form swollen blood vessels due to the failure to form a normal number of blood vessel branches (Huang et al., 2003), the *prp* mutation did not seem to rescue the branching defects of *reg6* at all (data not shown). Thus, plexus formation in *prp* is most likely due to defects in angiogenic patterning. However, we

NIH-PA Author Manuscript

NIH-PA Author Manuscript

NIH-PA Author Manuscript

were unable to determine from our present results whether collagen IX has a direct or indirect role in vascular plexus formation. In light of the fact that the *prp* mutation occurs in the thrombospondin domain which might bind to angiogenic cytokines and thus have a negative role in angiogenesis (Armstrong and Bornstein, 2003; Streit et al., 1999), we were tempted to hypothesize that col9α1 might directly regulate blood vessel pattering via an interaction of its thrombospondin domain with ECs. Nevertheless, it seems clear from our results that collagen IX plays a role in regulating vascular plexus formation, but elucidation of the mechanism requires further studies.

The role of collagen IX in ECM scaffolds

Our studies with the zebrafish *prp* mutation also led us to a more-detailed understanding of the roles of collagen IX in ECM assembly. During ECM assembly, collagen IX is known to serve as a bridge within and among collagen II and other fibrils (Diab et al., 1996). As collagen II fibrils are one of the abundant matrix materials of the ECM, defects in collagen IX would presumably cause deterioration or significantly weaken ECM integrity. This role of collagen IX was nicely demonstrated in studies using knockout mice for col9α1, which developed severe degeneration in the joints (Fässler et al., 1994) and in human intervertebral disc disease where col9α2 is mutated (Annunen et al., 1999). Our study with the zebrafish col9α1 mutation further strengthens this notion by showing the disintegrated collagen II fibrils in mutant fish (Figs. 5 and 6). In addition, our results provide more insights into ECM assembly involving collagen IX. First, we noted that not only were the affected collagen II fibrils broken in mutant fish, but their sizes varied and were dramatically smaller, suggesting that collagen IX is probably not required for the initial assembly but for the growth of collagen II fibrils. Although prp is a point mutation in the thrombospondin domain of col9α1, which is not known to have a critical role in the assembly of collagen II fibrils, our morpholino knockdown of the col9α1 gene seemed to suggest that the phenotype of *prp* mutants was close to the result of loss of function of col9α1 (Fig. 4). Second, collagen IX apparently is involved in collagen II patterning, as we observed abnormal orientations and mis-localization in the lepidotrichia of collagen II fibrils (Fig. 6). While these observations are still difficult to interpret, they suggest a possible role of collagen IX in connecting collagen II with other matrices. Finally, collagen IX also plays an important role in determining the size and shape of peripheral body parts, the caudal fin in the present case. *prp* mutants consistently exhibited small finfolds during early development. By the time of caudal fin development, the fin rays appeared wavy and had irregular intervals. Their fin segments were actually smaller, too (data not shown). All of these factors contributed to the very abnormal fin shapes of *prp* mutants which rendered the mutant fish easily identifiable. Furthermore, it is worth noting that both actinotrichia and lepidotrichia are types of dermal bones. Although it is still not clear whether the mechanisms for the assembly of the fin ECM structures are the same as those for the dermal bone formation in human such as skull, the zebrafish caudal fin clearly offers a simple in vivo model for the studies on dermal bone formation.

The ECM structures and vascular development in zebrafish caudal fins

The close proximity of the actinotrichia and the developing vasculature in the caudal fin tips suggests a possible direct interaction. In the growing fin tips, we observed very thin structure with only one layer of mesenchymal cell sandwiched by actinotrichia and epidermis (Fig. 5C). With the arrangement and the large number of actinotrichia in the fin tip, it is conceivable that the pioneer blood vessels growing into this region would very likely have direct contact with and be influenced by the actinotrichia. Our results that the vascular plexus phenotype of *prp* seems to specifically result from the actinotrichia defects provide supporting evidence to this notion (Figs. 7 and 8). In contrast, lepidotrichia seem less involved in the vascular development since it is formed at the more proximal level and

NIH-PA Author Manuscript

NIH-PA Author Manuscript

NIH-PA Author Manuscript

anatomically away from the blood vessels (Figs. 5A, B). To our best knowledge, no other reports have been able to demonstrate the specific connection between any collagen defect and vascular plexus formation.

The zebrafish young caudal fin system

As addressed earlier, interactions of ECs with the ECM and other tissues are often complex, and thus it is difficult to provide a clear view of causes vs. consequences. Although this seemed true in our study, we found that the young caudal fin system provides the following advantages for studying relationships of ECs with the ECM and neighboring tissues during development. First, our results reveal a very distinct morphological and cellular sequence of vascular and tissue development in young caudal fins (Fig. 9). Only very few cell types are present at the beginning of caudal fin development. As we demonstrated, epidermal cells first pattern the fin rays followed by the invasion of blood vessels which exhibit a very stereotypical process of patterning. Osteoblasts then array themselves following the vascular pattern. In addition, due to the thin tissue of the caudal fins, the cellular and extracellular phenotypes are very easy to analyze by whole mount, histological sections, or even electron microscopy. With these advantages, we were able to demonstrate that osteoblasts seem to closely follow the EC patterning in this peripheral body part (Fig. 7). The relationship between ECs and osteoblasts during development has not clearly been shown before. We also showed that axons of sensory neurons in the caudal fins seemed to pattern themselves independently of blood vessels (Fig. 8). Although this result seems to contradict a previous report from chickens (Mukouyama et al., 2002), we reasoned that it is possible that different parts of the body may have different developmental strategies.

Supplementary Material

Refer to Web version on PubMed Central for supplementary material.

Acknowledgments

We would like to thank the staff at the Core Facilities of the ICOB for their technical assistance. Special thanks go to Mr. HungKeng Chou for the artwork of Fig. 9. This work was supported by a Distinguished Postdoctoral Fellowship to C.C.H. from Academia Sinica and grant 94M011-1 from the Genomic Center, Academia Sinica.

References

Akimenko M, Johnson SL, Westerfield M, Ekker M. Differential induction of four msx homeobox genes during fin development and regeneration in zebrafish. Development. 1995; 121:347–357. [PubMed: 7768177]

Annunen S, Paassilta P, Lohiniva J, Perälä M, Pihlajamaa T, Karppinen J, Tervonen O, Kröger H, Lähde S, Vanharanta H, Ryhänen L, Göring H, Ott J, Prockop D, Ala-Kokko L. An allele of COL9A2 associated with intervertebral disc disease. Science. 1999; 285:409–412. [PubMed: 10411504]

Aplin AE, Short SM, Juliano RL. Anchorage-dependent regulation of the mitogen-activated protein kinase cascade by growth factors is supported by a variety of integrin alpha chains. J. Biol. Chem. 1999; 274:31223–31228. [PubMed: 10531317]

Armstrong LC, Bornstein P. Thrombospondins 1 and 2 function as inhibitors of angiogenesis. Matrix[?]. Biol. 2003; 22:63–71.

Bork P. The modular architecture of vertebrate collagens. FEBS Lett. 1992; 307:49–54. [PubMed: 1639194]

Canty E, Kadler K. Procollagen trafficking, processing and fibrillogenesis. J. Cell. Sci. 2005; 118:1341–1353. [PubMed: 15788652]

Carmeliet P. Angiogenesis in life, disease and medicine. Nature. 2005; 438:932–936. [PubMed: 16355210]

NIH-PA Author Manuscript

NIH-PA Author Manuscript

NIH-PA Author Manuscript

Cleaver O, Melton D. Endothelial signaling during development. Nat. Med. 2003; 9:661–668. [PubMed: 12778164]

Crivellato E, Nico B, Ribatti D. Contribution of endothelial cells to organogen-esis: a modern reappraisal of an old Aristotelian concept. J. Anat. 2007; 211:415–427. [PubMed: 17683480]

Davis G, Senger D. Endothelial extracellular matrix: biosynthesis, remodeling, and functions during vascular morphogenesis and neovessel stabilization. Circ. Res. 2005; 97:1093–1107. [PubMed: 16306453]

Diab M, Wu J, Eyre D. Collagen type IX from human cartilage: a structural profile of intermolecular cross-linking sites. Biochem. J. 1996; 314(Pt. 1):327–332. [PubMed: 8660302]

Du S, Frenkel V, Kindschi G, Zohar Y. Visualizing normal and defective bone development in zebrafish embryos using the fluorescent chromophore calcein. Dev. Biol. 2001; 238:239–246. [PubMed: 11784007]

Eyre D, Weis M, Wu J. Articular cartilage collagen: an irreplaceable framework? Eur. Cells. Mater. 2006; 12:57–63.

Ferrara N, Kerbel R. Angiogenesis as a therapeutic target. Nature. 2005; 438:967–974. [PubMed: 16355214]

Fässler R, Schnegelsberg P, Dausman J, Shinya T, Muragaki Y, McCarthy M, Olsen B, Jaenisch R. Mice lacking alpha 1 (IX) collagen develop noninflammatory degenerative joint disease. Proc. Natl. Acad. Sci. U.S.A. 1994; 91:5070–5074. [PubMed: 8197187]

Huang C, Lawson N, Weinstein B, Johnson S. reg6 is required for branching morphogenesis during blood vessel regeneration in zebrafish caudal fins. Dev. Biol. 2003; 264:263–274. [PubMed: 14623247]

Johanson Z, Burrow C, Warren A, Carvey J. Homology of fin lepidotrichia in osteichthyan fishes. Lethaia. 2005; 38:27–36.

Johnson SL, Midson CN, Ballinger EW, Postlethwait JH. Identification of RAPD primers that reveal extensive polymorphisms between laboratory strains of zebrafish. Genomics. 1994; 19:152–156. [PubMed: 8188217]

Lammert E, Cleaver O, Melton D. Induction of pancreatic differentiation by signals from blood vessels. Science. 2001; 294:564–567. [PubMed: 11577200]

Lawson N, Weinstein B. In vivo imaging of embryonic vascular development using transgenic zebrafish. Dev. Biol. 2002; 248:307–318. [PubMed: 12167406]

Lecuit T, Le Goff L. Orchestrating size and shape during morphogenesis. Nature. 2007; 450:189–192. [PubMed: 17994084]

Mabee PM. Supraneural and predorsal bones in fishes: development and homologies. Copeia. 1988; 1988:827–838.

Margosio B, Marchetti D, Vergani V, Giavazzi R, Rusnati M, Presta M, Taraboletti G. Thrombospondin 1 as a scavenger for matrix-associated fibroblast growth factor 2. Blood. 2003; 102:4399–4406. [PubMed: 12947001]

Meinhardt H. Models of biological pattern formation: from elementary steps to the organization of embryonic axes. Curr. Top. Dev. Biol. 2008; 81:1–63. [PubMed: 18023723]

Meredith JE, Schwartz MA. Integrins, adhesion and apoptosis. Trends Cell. Biol. 1997; 7:146–150. [PubMed: 17708932]

Montesano R, Orci L, Vassalli P. In vitro rapid organization of endothelial cells into capillary-like networks is promoted by collagen matrices. J. Cell. Biol. 1983; 97:1648–1652. [PubMed: 6630296]

Mukouyama Y, Shin D, Britsch S, Taniguchi M, Anderson D. Sensory nerves determine the pattern of arterial differentiation and blood vessel branching in the skin. Cell. 2002; 109:693–705. [PubMed: 12086669]

Paassilta P, Lohiniva J, Göring H, Perälä M, Räinä S, Karppinen J, Hakala M, Palm T, Kröger H, Kaitila I, Vanharanta H, Ott J, Ala-Kokko L. Identification of a novel common genetic risk factor for lumbar disk disease. JAMA. 2001; 285:1843–1849. [PubMed: 11308397]

Rahman S, Patel Y, Murray J, Patel KV, Sumathipala R, Sobel M, Wijelath ES. Novel hepatocyte growth factor (HGF) binding domains on fibronectin and vitronectin coordinate a distinct and

NIH-PA Author Manuscript

NIH-PA Author Manuscript

NIH-PA Author Manuscript

amplified met-integrin induced signalling pathway in endothelial cells. BMC Cell. Biol. 2005; 6:8. [PubMed: 15717924]

Ruehl M, Somasundaram R, Schoenfelder I, Farndale RW, Knight CG, Schmid M, Ackermann R, Riecken EO, Zeitz M, Schuppan D. The epithelial mitogen keratinocyte growth factor binds to collagens via the consensus sequence glycine– proline–hydroxyproline. J. Biol. Chem. 2002; 277:26872–26878. [PubMed: 11973338]

Senger DR, Perruzzi CA, Streit M, Koteliansky VE, de Fougerolles AR, Detmar M. The alpha1beta1 and alpha2beta1 integrins provide critical support for vascular endothelial growth factor signaling, endothelial cell migration, and tumor angiogenesis. Am. J. Pathol. 2002; 160:195–204. [PubMed: 11786413]

Singer A, Perlman H, Yan Y, Walker C, Corley-Smith G, Brandhorst B, Postlethwait J. Sex-specific recombination rates in zebrafish (*Danio rerio*). Genetics. 2002; 160:649–657. [PubMed: 11861568]

Solnica-Krezel L, Schier A, Driever W. Efficient recovery of ENU-induced mutations from the zebrafish germline. Genetics. 1994; 136:1401–1420. [PubMed: 8013916]

Streisinger G, Walker C, Dower N, Knauber D, Singer F. Production of clones of homozygous diploid zebra fish (*Brachydanio rerio*). Nature. 1981; 291:293–296. [PubMed: 7248006]

Streit M, Riccardi L, Velasco P, Brown LF, Hawighorst T, Bornstein P, Detmar M. Thrombospondin-2: a potent endogenous inhibitor of tumor growth and angiogenesis. Proc. Natl. Acad. Sci. U.S.A. 1999; 96:14888–14893. [PubMed: 10611308]

Westerfield, M. The Zebrafish Book. A Guide for the Laboratory Use of Zebrafish (*Danio rerio*). Eugene, OR: University of Oregon Press; 2000.

Whelan MC, Senger R. Collagen I initiates endothelial cell morphogenesis by inducing actin polymerization through suppression of cyclic AMP and protein kinase A. J. Biol. Chem. 2003; 278:327–334. [PubMed: 12399469]

Wijelath ES, Murray J, Rahman S, Patel Y, Ishida A, Strand K, Aziz S, Cardona C, Hammond WP, Savidge GF, Rafii S, Sobel M. Novel vascular endothelial growth factor binding domains of bigronectin enhance vascular endothelial growth factor biological activity. Circ. Res. 2002; 91:25–31. [PubMed: 12114318]

Wood A, Thorogood P. An analysis of in vivo cell migration during teleost fin morphogenesis. J. Cell. 1984; 66:205–222.

NIH-PA Author Manuscript
NIH-PA Author Manuscript
NIH-PA Author Manuscript

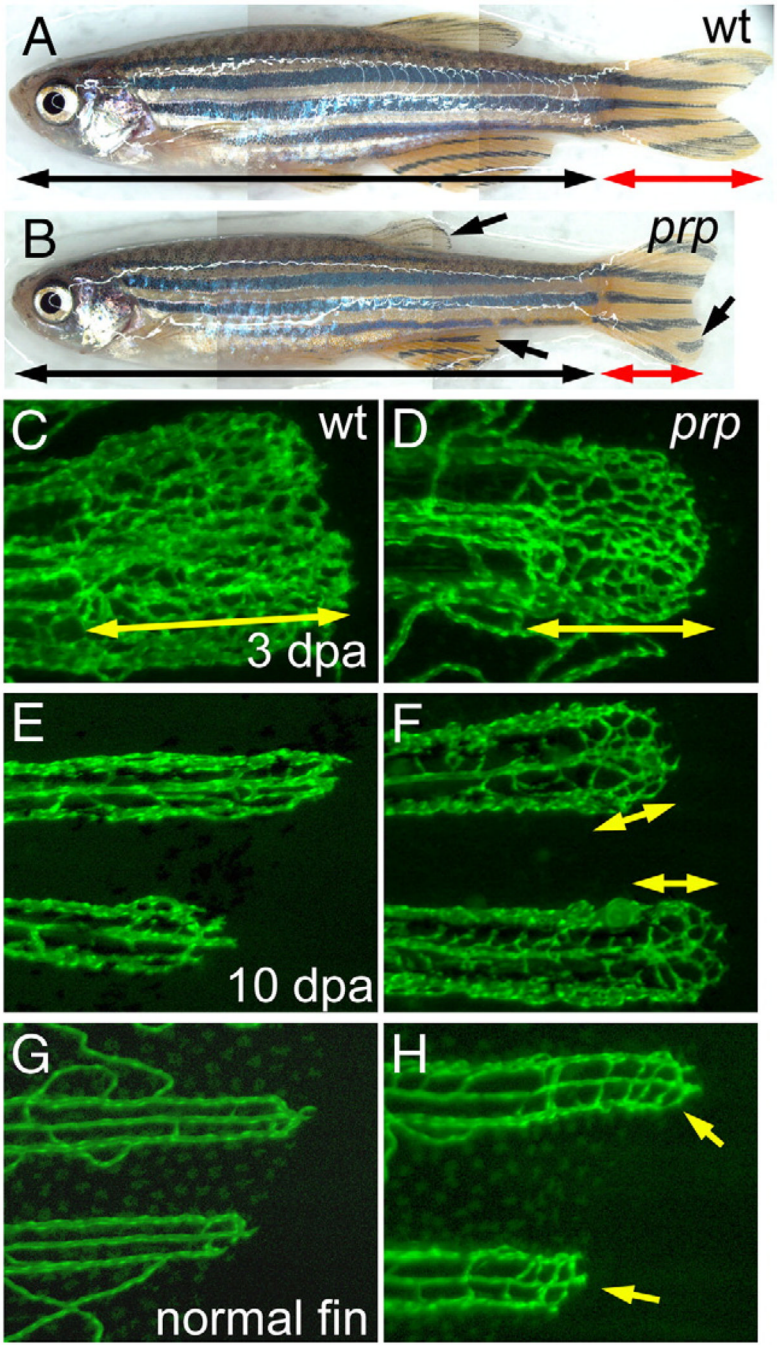

Fig. 1.

Persistent formation of vascular plexuses in ontogenetic and regenerating blood vessels in zebrafish *prp* mutants. (A) Wild-type (WT) and (B) *prp* adult zebrafish showing that the *prp* mutant has a normal body but smaller fins with rounded edges (arrows). (C) to (F) Regenerating experiments of fish after amputation. (C) A representative 3-day post-amputation (dpa) regenerating fin ray of the WT showing the vascular plexus at the fin tip (double-headed arrow). (D) Vascular plexuses seemed to form normally in *prp* 3-dpa regenerating fins (double-headed arrow). (E) At 10 dpa, fin vessels continued to regenerate without forming a plexus in the WT. (F) In the *prp* mutant, vascular plexuses (double-headed arrows), however, were still present in the 10-dpa regenerating fins. (G, H) WT and

prp mutant fish. (G) The vascular plexus is normally not seen at the tips of normal WT fins. (H) In contrast, at almost every tip of a normal *prp* fin, a plexus-like vascular network could easily be detected (arrows).

NIH-PA Author Manuscript
NIH-PA Author Manuscript
NIH-PA Author Manuscript

NIH-PA Author Manuscript
NIH-PA Author Manuscript
NIH-PA Author Manuscript

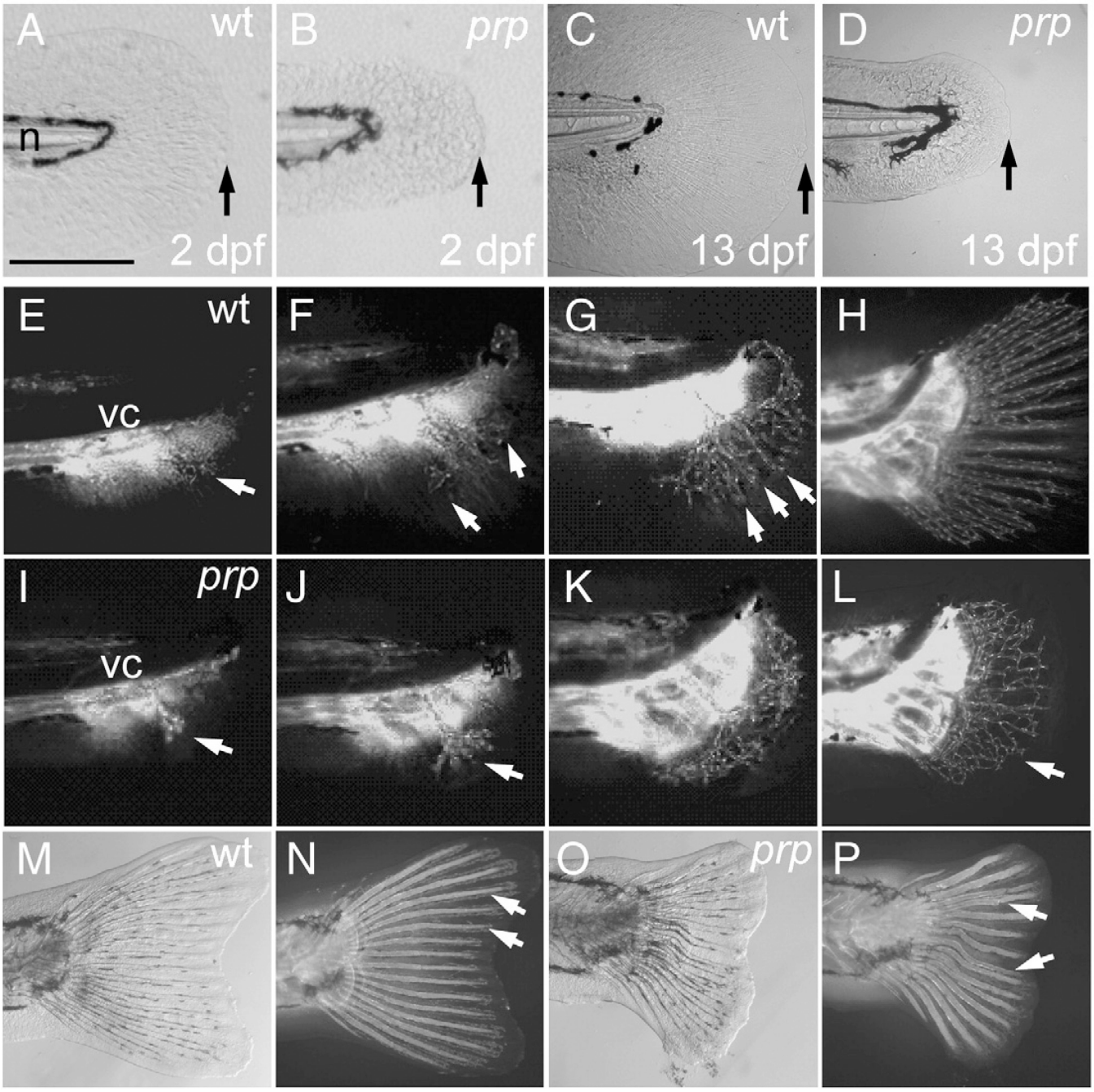

Fig. 2.

Small finfold and vascular plexus in young caudal fins of *prp* mutants. (A) Wild-type (WT) and (B) *prp* 2 day post-fertilization (dpf) embryos showing the small-finfold phenotype in *prp*. (C) WT and (D) *prp* larvae, at ~13 dpf, showing the small-finfold phenotype throughout the larval stage in *prp*. Arrows in panels A–D denote the distal edges of the caudal finfolds. n, notochord. (E–H) Time lapse images of the developing vasculature between around 20 and 40 dpf in a WT caudal fin. (E) Fin vessels (arrow) growing from the posterior ends of axial vessels located below the vertebral column (vc). (F) Pioneer vessels (arrows) branching and growing dorsally and ventrally. (G) Fin vessels were organized into a radial pattern (arrows) soon after the vessels grow into the caudal fin. (H) Within a week, the

NIH-PA Author Manuscript

NIH-PA Author Manuscript

NIH-PA Author Manuscript

mature 16–18-ray pattern of the fin vasculature was established. (I–L) Early development of the caudal fin vasculature in a representative *prp* mutant. (I, J) Pioneer fin vessels (arrows) growing out and branching normally in *prp* fish. (K, L) Instead of forming a radial pattern, the fin vessels of the *prp* mutant formed a large vascular plexus which expanded into the entire caudal fin (arrow in L). (M, bright light; N, fluorescence) In WT fish, the bony fin rays or lepidotrichia were stained by calcein fluorescent dye (arrows; Du et al., 2001) and were organized into a radial pattern associated with the vessels. (O, bright light; P, fluorescence) Fin rays of the *prp* mutant were often curved and juxtaposed and even fused (arrows). Anterior, left; dorsal top. Scale bars, 150 μm for panels A–D.

NIH-PA Author Manuscript
NIH-PA Author Manuscript
NIH-PA Author Manuscript

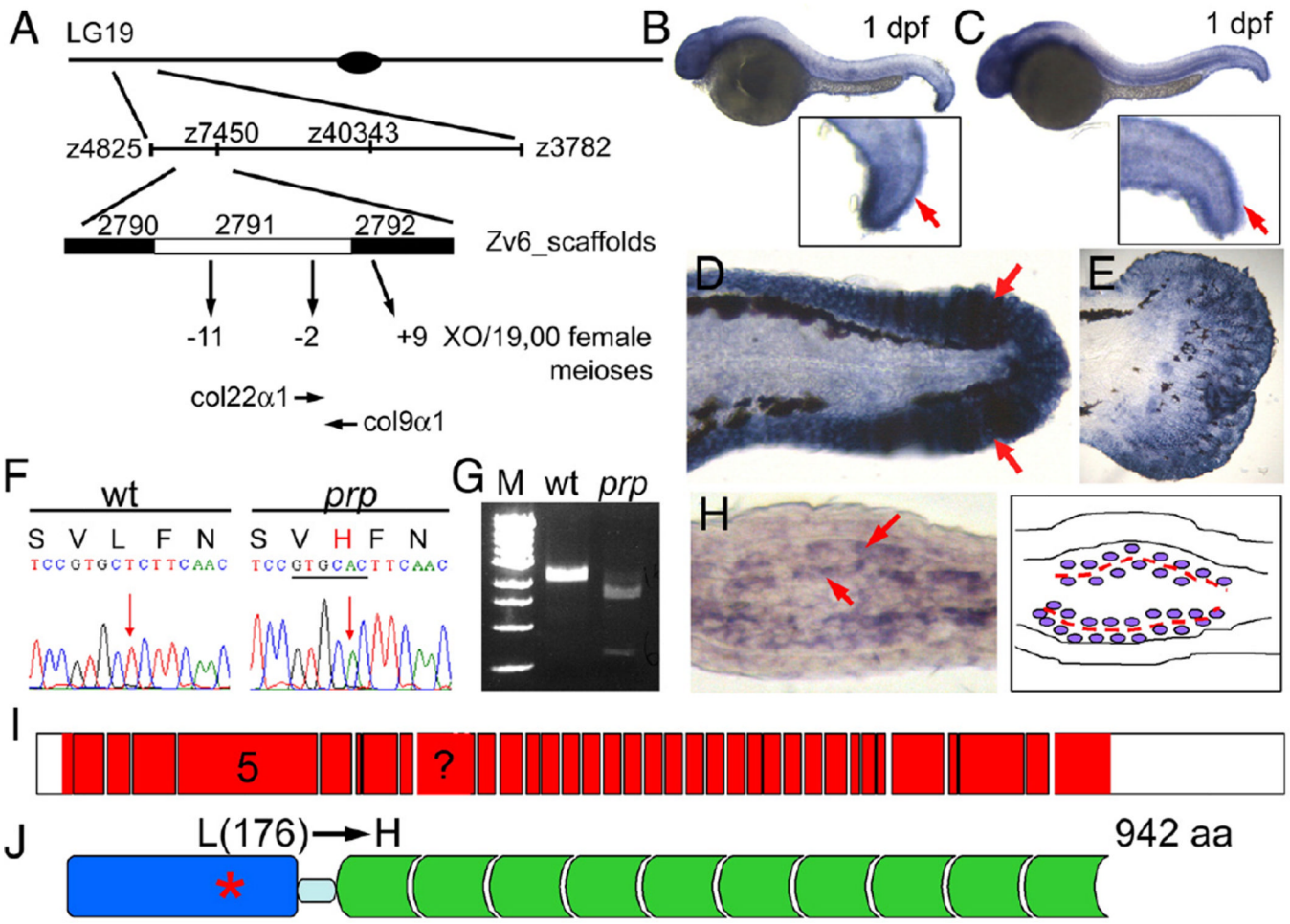

Fig. 3.

prp encodes the zebrafish col9α1. (A) Positional cloning of *prp*. Top, Chromosomal view of the location of *prp*. Areas are not drawn to scale. (B) col9α1 and (C) col22α1 were found to be expressed in 1-day post-fertilization (dpf) embryonic finfolds (arrows) by in situ hybridization. (D) col9α1 was also highly expressed in the finfold of a 2-dpf embryo and (E) the developing caudal fin of a 15-dpf larva. Anterior, left; dorsal top. (F)AT-to-A single nucleotide change was detected in the col9α1 gene of *prp* which created a restriction enzyme site for ApaLI (underlined) and caused a leucine (L) to change to histidine (H). (G) RT-PCR products covering the mutation site of *prp* were digested by ApaLI. M, DNA markers. (H) A cross-section of a regenerating fin showing that col9α1 was expressed in cells that sandwich the forming actinotrichia (arrows; further described in Figs. 5 and 6). (I) An intron–exon map showing that col9α1 is composed of at least 36 exons (red boxes) and untranslated regions (UTRs) (white boxes). Exon 5 encodes the thrombospondin domain, where the *prp* mutation is found, and is also what the morpholino was designed to delete. The exon with a question mark was not clearly resolved due to a lack of a genomic sequence in this region. (J) The protein structure of zebrafish COL9α1. The protein is 942-amino-acid long and contains a thrombospondin domain (blue) on the N terminus and a long stretch of glycine-X–Y repeats (green) separated by a small gap (light blue). The *prp* mutation resulted in an amino-acid change from leucine (176) to histidine in the thrombospondin domain of COL9α1.

NIH-PA Author Manuscript

NIH-PA Author Manuscript

NIH-PA Author Manuscript

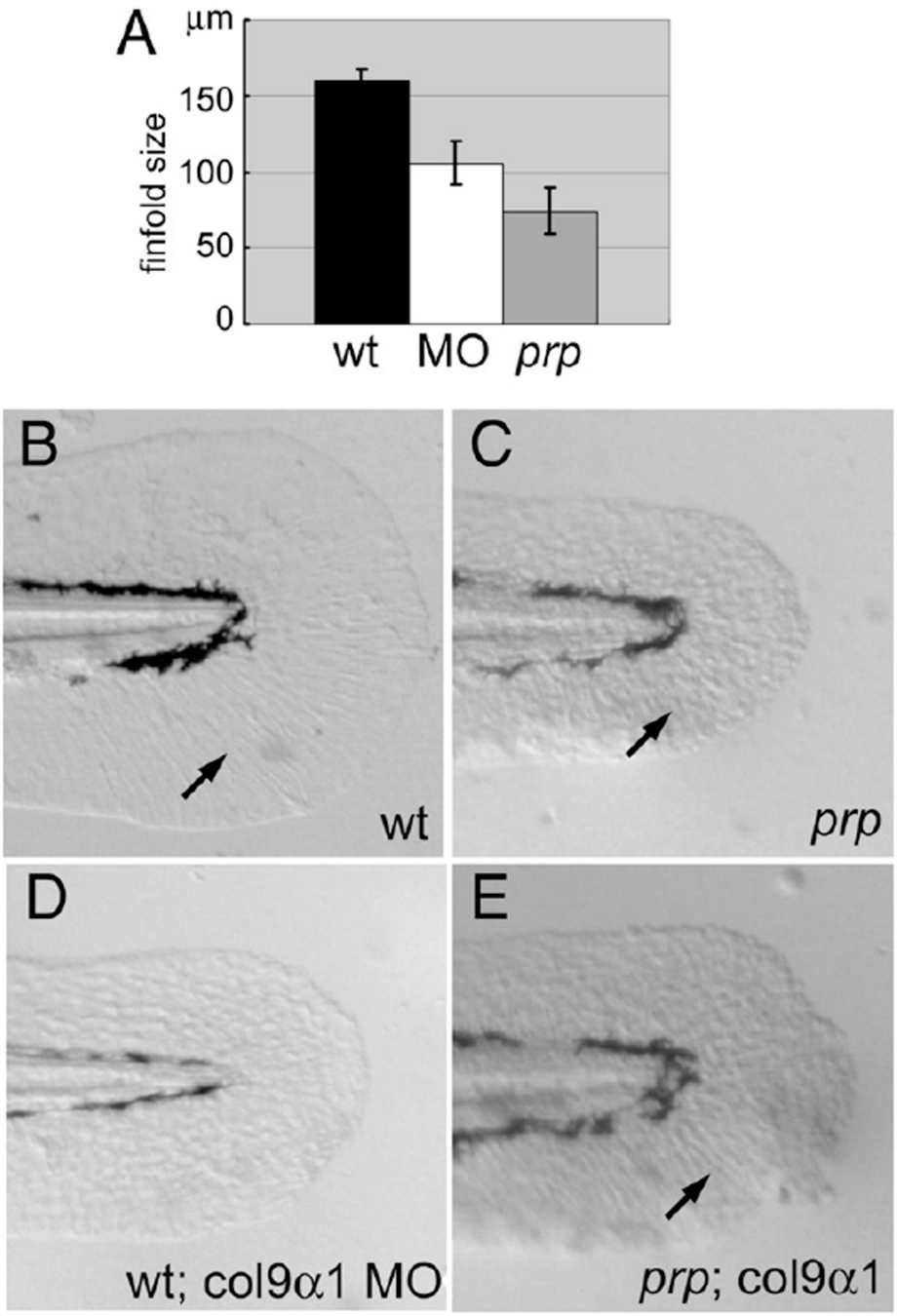

Fig. 4.

Col9α1 morpholino phenocopies the *prp* finfold phenotype while overexpression of col9α1 rescues *prp*. (A) A gene-specific morpholino (MO) targeting the splice site of col9α1 exon 5 caused the small-finfold phenotype in wild-type (WT) embryos. (B) The tail of a 2-day post-fertilization (dpf) uninjected WT embryo showing a normal finfold with radial actinotrichia (arrow). (C) A *prp* embryo showing a small finfold with short and sparse actinotrichia (arrow). (D) A WT embryo injected with the col9α1 MO developed the *prp*-like small-finfold and actinotrichia defects. (E) A *prp* embryo injected with the col9α1 plasmid developed a mosaic finfold with a *prp*-like portion in the dorsal half and a normal-looking

portion in the ventral half where normal actinotrichia can be seen (arrow). Arrows, actinotrichia. Anterior, left; dorsal top.

NIH-PA Author Manuscript
NIH-PA Author Manuscript
NIH-PA Author Manuscript

NIH-PA Author Manuscript

NIH-PA Author Manuscript

NIH-PA Author Manuscript

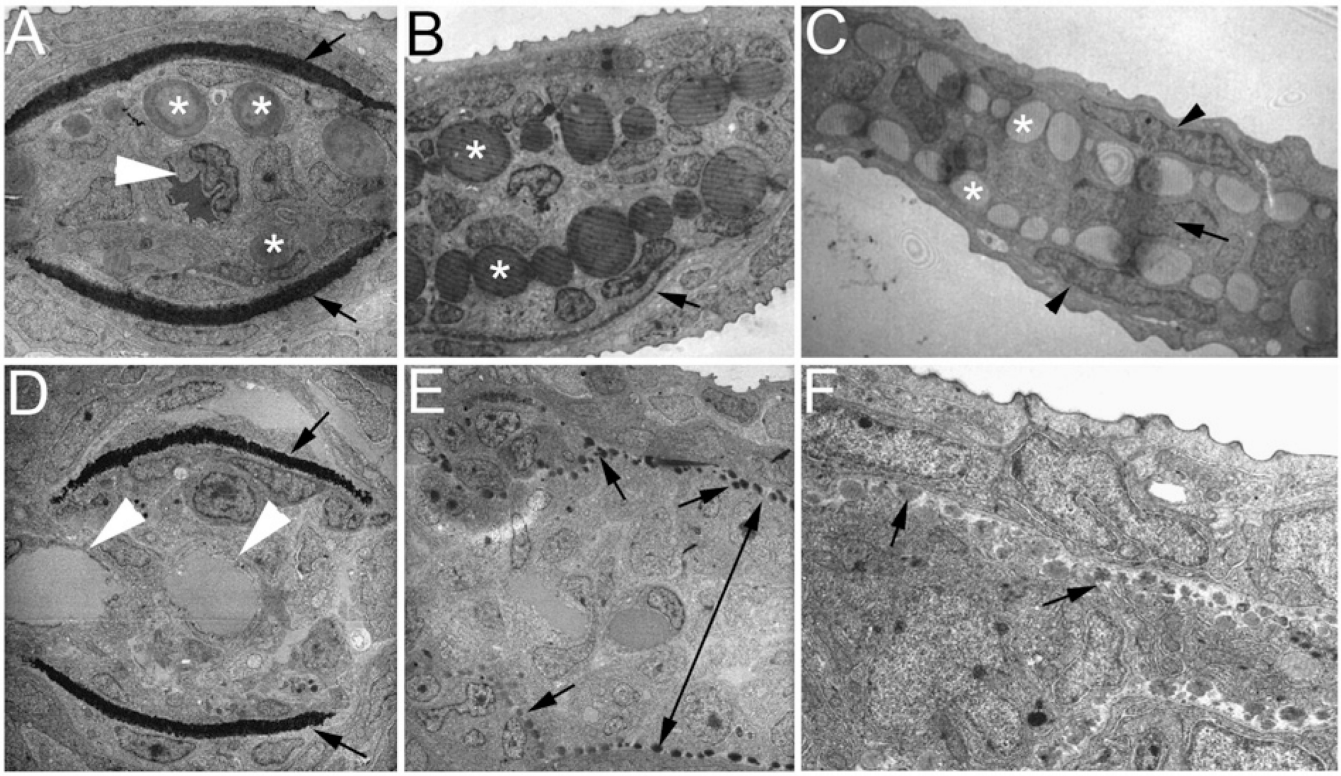

Fig. 5.

Ultrastructural analyses of zebrafish caudal fins by TEM. (A–C) Wild-type (WT) fin sections showing the structural organization of the fin tip. (A) In a proximal section, the lepidotrichia hemirays were stained dark (arrows) and actinotrichia are large bundles located inside near the hemirays (asterisks). A single artery can be seen in the center of the fin ray (arrowhead). (B) In a medial section, actinotrichial bundles were prominent (asterisks), but lepidotrichia were thin (arrow, only one side of the lepidotrichia is shown in this section). (C) In a distal section, the fin was much thinner and consisted of only the outer layers of the epidermis (arrowheads), numerous actinotrichia bundles (asterisks), and a one-cell layer of the mesenchyme (arrow). (D–F) Sections of a *prp* fin tip. (D) In a proximal section, the lepidotrichia hemirays are visible (arrows), but the actinotrichia were not present. Also in this section, two vessels can be observed in the intra-ray compartment (arrowheads) reflecting the plexus phenotype of *prp*. (E) In a medial section, actinotrichial bundles are visible but much smaller at almost the size of dots (arrows). Interestingly, the mesenchymal compartment was thicker in *prp* (double-headed arrow). (C) In a distal section, the actinotrichia were again small, and the intra-ray mesenchymal compartment was thick in *prp*. Note that one cannot directly compare the sizes of actinotrichia in (E) and (F) because they are of different magnifications.

NIH-PA Author Manuscript
NIH-PA Author Manuscript
NIH-PA Author Manuscript

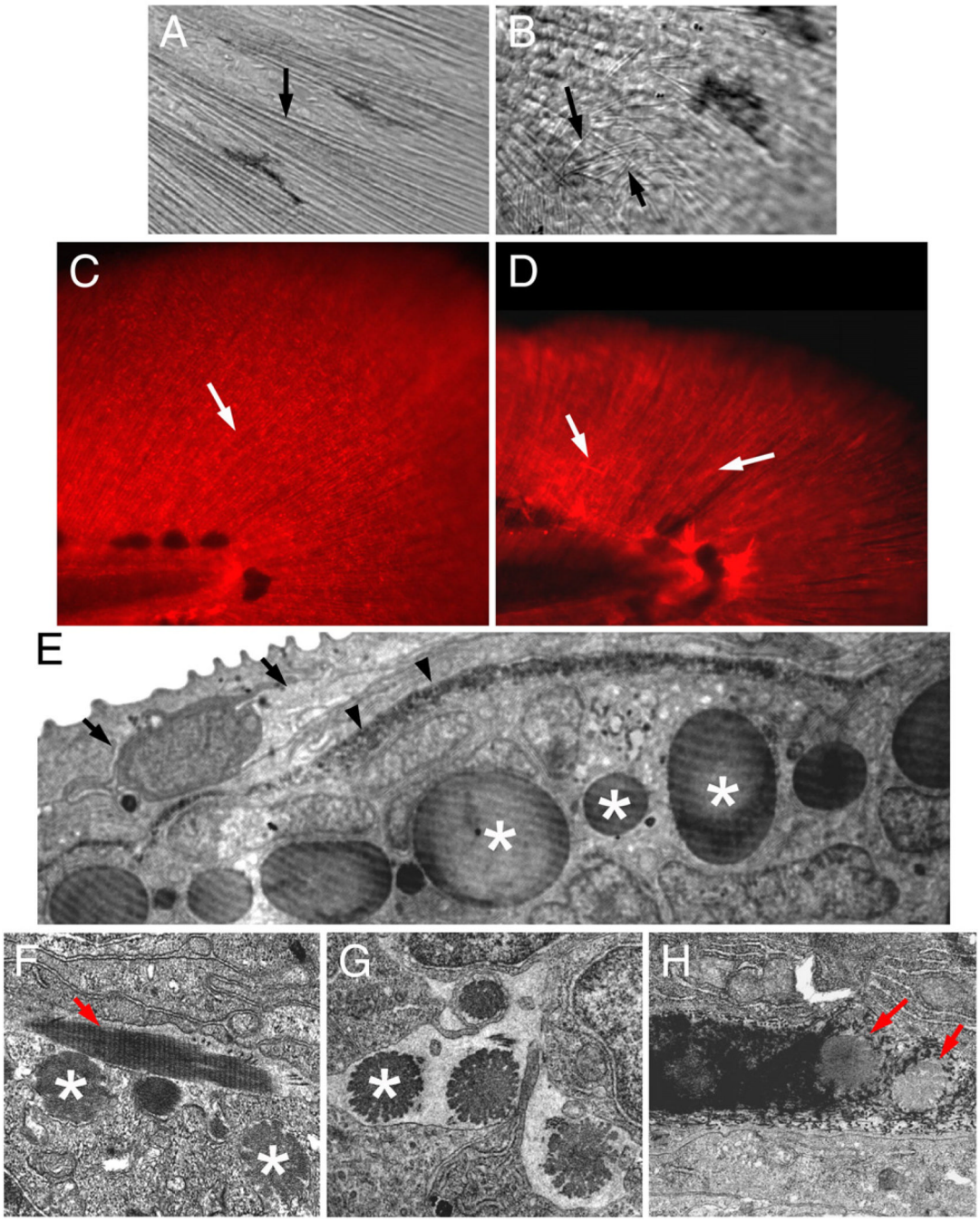

Fig. 6.

Actinotrichia defects in *prp* mutants. Bright light examination of (A) wild-type (WT) and (B) *prp* finfolds revealed short and mis-orientated actinotrichia in *prp* (arrows). (C, D) Immunostaining of zebrafish finfolds with a monoclonal antibody against human collagen II. (C) In the WT finfold, this antibody stained the actinotrichia (arrows). (D) In *prp*, however, the actinotrichia appeared less dense and were often crisscrossed (arrows). (E) Analyses with transmission electronic microscopy (TEM) showed that in the WT fin, actinotrichia (asterisks) were bundles of collagen matrices located beneath the epidermis (arrow) and lepidotrichia (arrowheads). (F–H) The actinotrichia of the *prp* mutant appeared

broken and much smaller (asterisks), sometimes perpendicular (arrow in panel F), and misassembled within the lepidotrichia (arrow in panel H).

NIH-PA Author Manuscript
NIH-PA Author Manuscript
NIH-PA Author Manuscript

NIH-PA Author Manuscript
NIH-PA Author Manuscript
NIH-PA Author Manuscript

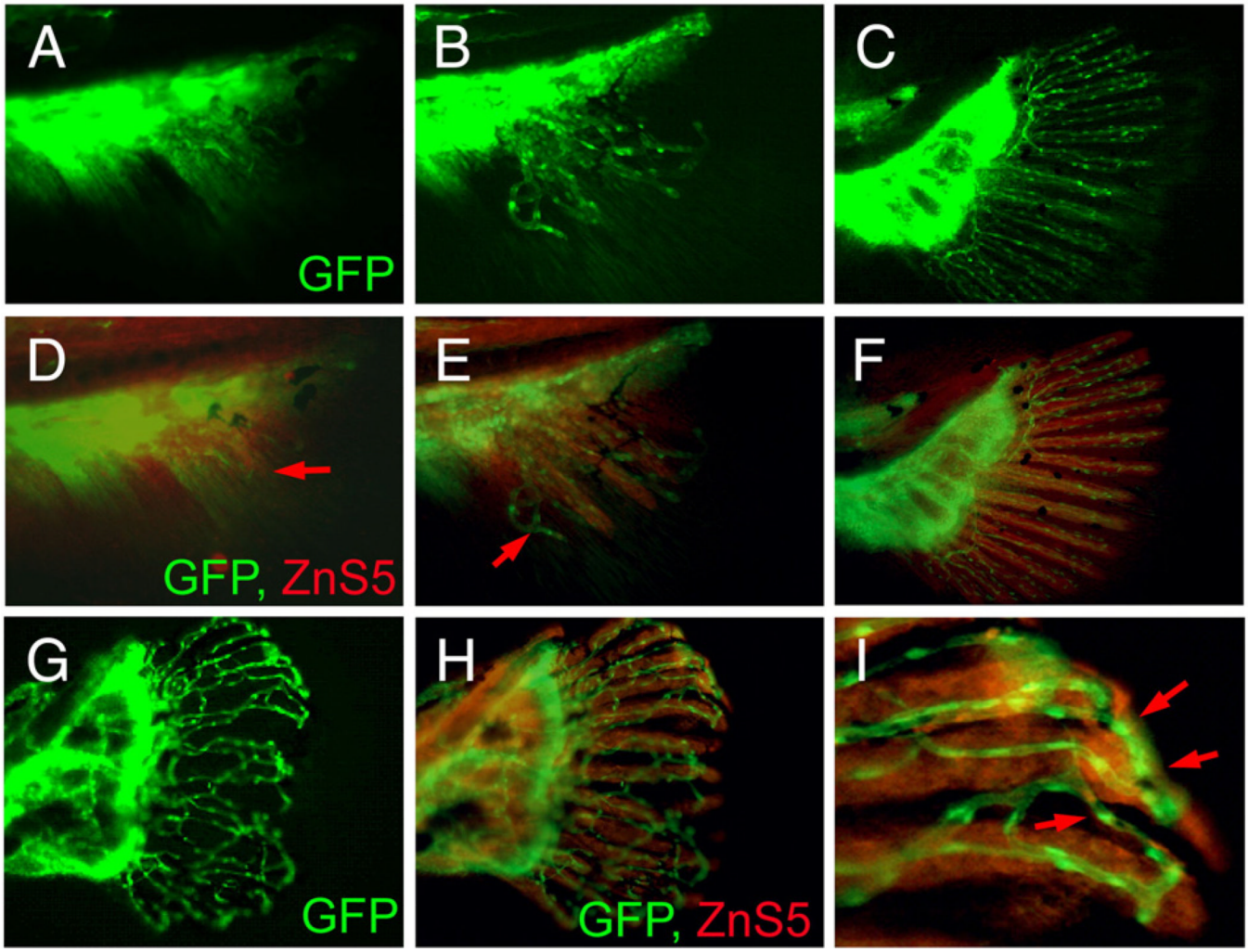

Fig. 7.

Vascular plexus causes wavy and fused fin rays in *prp* fish. (A–C) Blood vessel development in the caudal fin of wild-type (WT) fish. (D–F) Immunostaining of osteoblasts (red) with the ZnS5 monoclonal antibody of the same fins revealed that osteoblasts developed and were patterned after blood vessels asevidenced byareas where only blood vessels were present (arrows in panels D and E). (G) A *prp* fin showing the vascular plexus. (H) The same *prp* fin stained with ZnS5 (red) showing that the osteoblast pattern was closely associated with the blood vessel pattern. (I) High magnification of a representative area of (H) showing wavy and fused osteoblast rays along with the misconnected blood vessels (arrows).

NIH-PA Author Manuscript
NIH-PA Author Manuscript
NIH-PA Author Manuscript

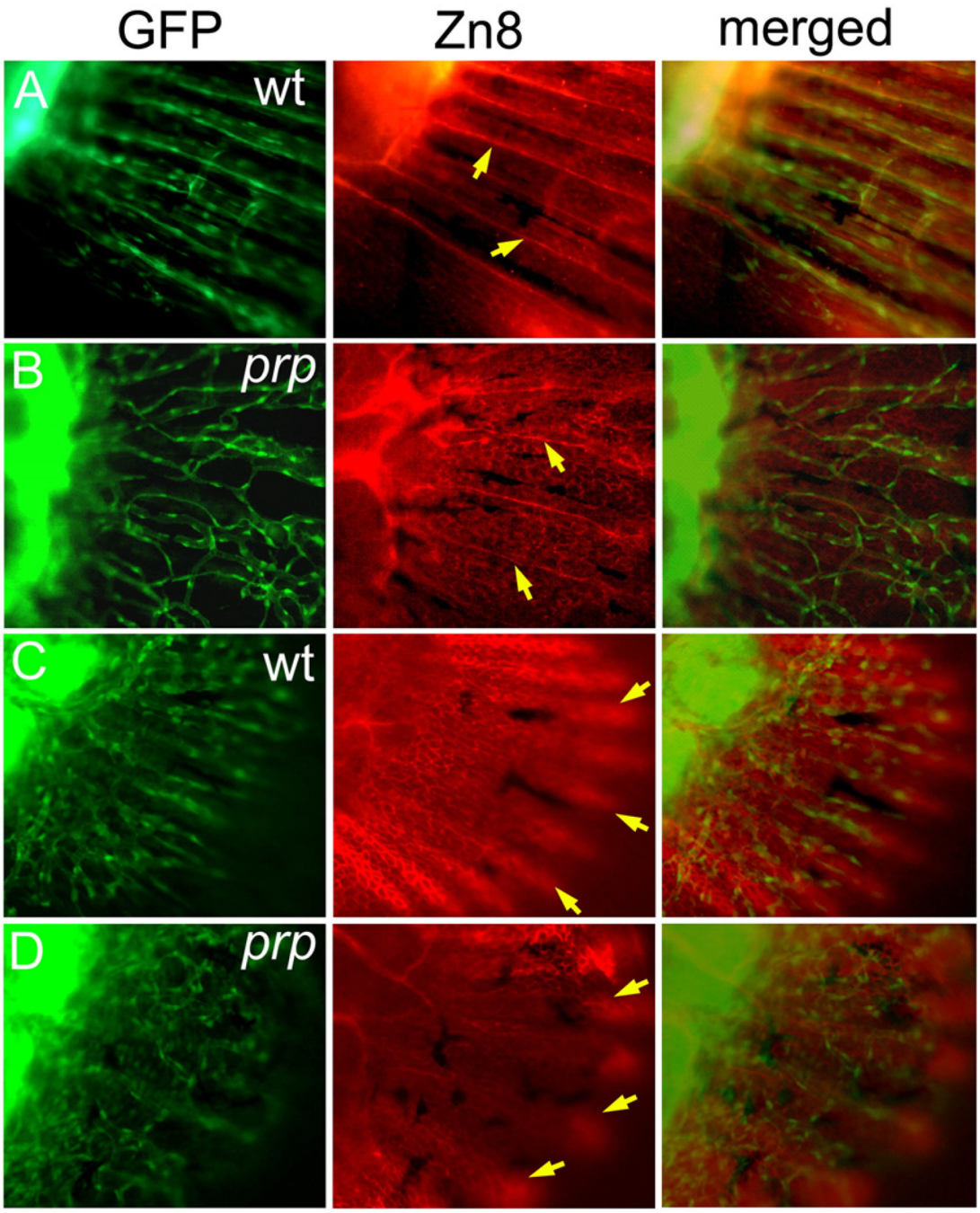

Fig. 8.

Independent developmental relationship between blood vessels, sensory axons, and the epidermis in a zebrafish caudal fin. (A) A wild-type (WT) fin stained with the Zn8 monoclonal antibody showing the sensory neuronal pattern in the fin. A single axon was found to extend along each fin ray (arrows). (B) In the *prp* mutant, the sensory axons maintained their ray pattern (arrows) and did not seem to be associated with the vascular plexus pattern. (C) AWT young fin stained with Zn8 and photographed with the focus on the epidermis showing that the epidermis formed a nice fin ray pattern (arrows). (D) A *prp* young fin showing that the epidermal pattern appeared relatively normal (arrows).

NIH-PA Author Manuscript

NIH-PA Author Manuscript

NIH-PA Author Manuscript

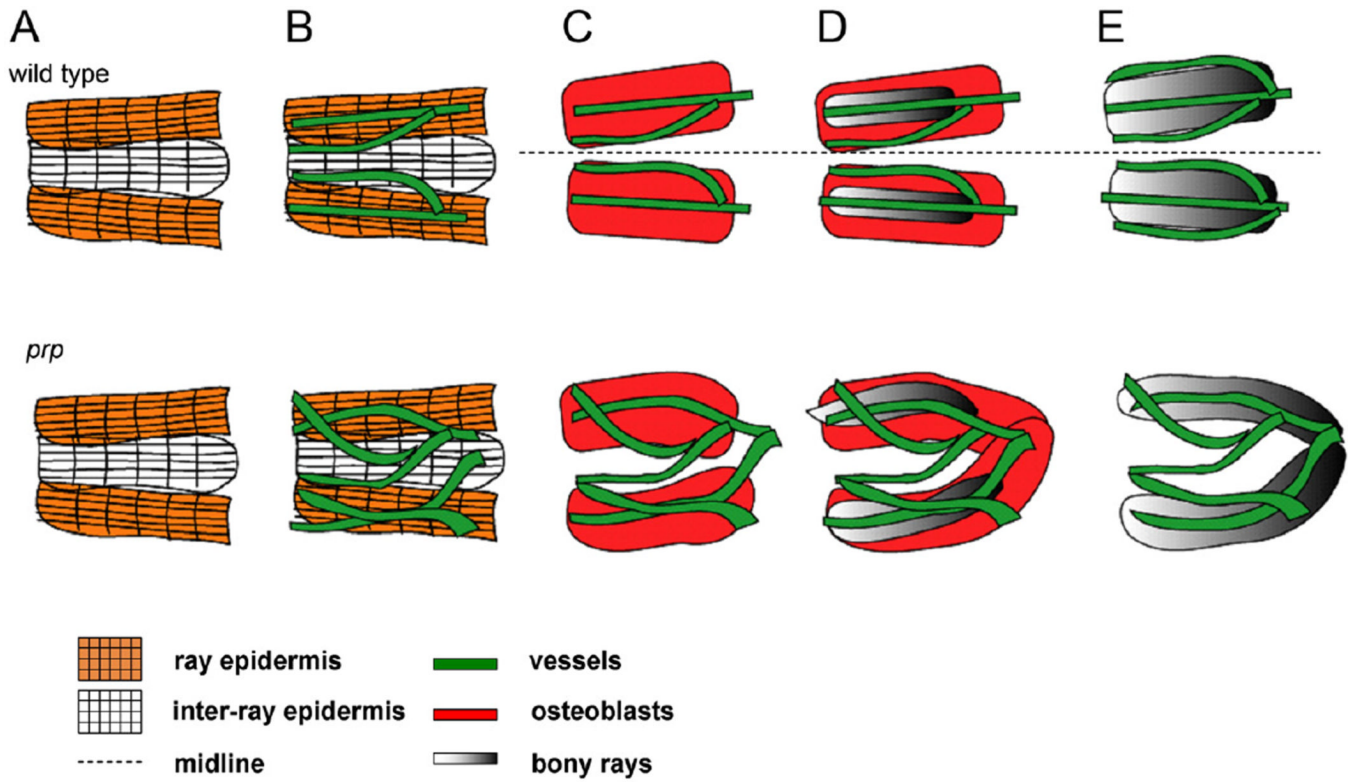

Fig. 9.

Model for developmental relationships between tissues in the young caudal fin. Upper row, wild-type (WT). (A) At the beginning of caudal fin development, the epidermis (as grids) first establishes the fin ray pattern (only two fin rays at midline are shown). The ray epidermis can be distinguished by the Zn8 antibody (orange grid). (B) Then, blood vessels (green) grow into the caudal fin and form the ray pattern which apparently follows the ray pattern established by the epidermis. At this stage, only two vessels are found in each fin ray, with one located in the center and the other outside but adjacent to the fin ray. (C) Soon after the blood vessels establish the ray pattern, osteoblasts form rays which are as wide as the future fin ray (red boxes) associated with the blood vessels. The epidermis is not shown. (D) Osteoblasts then begin to deposit the ray matrix (gray boxes). (E) Mature fin rays form, and within each one, three blood vessels can be found. Both the epidermis and osteoblasts were omitted for simplicity. Lower row, *prp* mutant. (A) The early epidermis development seems normal. (B) Soon after blood vessels grow into the caudal fin, they form plexuses. (C) Osteoblasts follow the blood vessel pattern and are often misconnected or fused (D). (E) The fin rays eventually become wavy and/or fused.